

Mediterranean Marine Science

Vol 15, No 3 (2014)

Vol 15, No 3 (2014)



Sea urchin response to rising pCO₂ shows ocean acidification may fundamentally alter the chemistry of marine skeletons

L. BRAY, M.A. PANCUCCI-PAPADOPOULOU, J. M. HALL-SPENCER

doi: [10.12681/mms.579](https://doi.org/10.12681/mms.579)

To cite this article:

BRAY, L., PANCUCCI-PAPADOPOULOU, M., & HALL-SPENCER, J. M. (2014). Sea urchin response to rising pCO₂ shows ocean acidification may fundamentally alter the chemistry of marine skeletons. *Mediterranean Marine Science*, 15(3), 510–519. <https://doi.org/10.12681/mms.579>

Sea urchin response to rising $p\text{CO}_2$ shows ocean acidification may fundamentally alter the chemistry of marine skeletons

L. BRAY^{1,2}, M. A. PANCUCCI-PAPADOPULOU² and J. M. HALL-SPENCER¹

¹ Marine Biology and Ecology Research Centre/Marine Institute, School of Marine Science & Engineering, University of Plymouth, Plymouth PL4 8AA, UK

² Institute of Oceanography, Hellenic Centre for Marine Research, 46,7 km Athens, Sounio Ave. P.O. Box 712, P.C. 19013 Anavyssos, Attiki, Greece

Corresponding author: laura.bray@plymouth.ac.uk

Handling Editor: Argyro Zenetos

Received: 8 August 2013; Accepted: 5 February 2014; Published on line: 25 April 2014

Abstract

Ocean acidification caused by an increase in $p\text{CO}_2$ is expected to affect marine ecosystem composition drastically, yet there is much uncertainty about the mechanisms through which ecosystems may be affected. Here we present the results of a study on sea urchins that are common and important grazers in the Mediterranean (*Paracentrotus lividus* and *Arbacia lixula*). Our study included a natural CO_2 seep plus reference sites in the Aegean Sea, Greece. The distribution of *A. lixula* was unaffected by the low pH environment, whereas densities of *P. lividus* were much reduced. There was skeletal degradation in both species living in acidified waters compared to reference sites and remarkable increases in skeletal manganese levels (541% increase for *P. lividus*, 243% increase for *A. lixula*), presumably due to changes in mineral crystalline structure. Levels of strontium and zinc were also altered. It is not yet known whether such dramatic changes in skeletal chemistry will affect coastal systems but our study reveals a mechanism that may alter inter-species interactions.

Keywords: Skeletal mineralogy, *Paracentrotus lividus*, *Arbacia lixula*, ocean acidification, CO_2 seeps.

Introduction

Ocean acidification, caused by an increase in $p\text{CO}_2$, is expected to affect the composition of marine ecosystems drastically (Zeebe, 2012), yet there is great uncertainty about how key ecosystem engineers will respond to the rapid rate of chemical change in ocean surfaces. Here we studied the effects of increased $p\text{CO}_2$ on sea urchins, which are important for three main reasons. Firstly, they are often keystone species in shallow rocky shore ecosystems since their grazing can structure communities affecting commercially important crustaceans and fish (Sala *et al.*, 1998); secondly, they contribute an estimated 66.7 g $\text{CaCO}_3 \text{ m}^{-2} \text{ y}^{-1}$ to annual oceanic CaCO_3 production, thus influencing global bio-geochemical cycles (Lebrato *et al.*, 2010); and thirdly, they support a fishing industry worth approximately 89 million US dollars (FAOSTAT, 2013).

Sea urchins have an acid-base physiology that is less able to cope with elevated $p\text{CO}_2$ than many other groups of marine organisms (Miles *et al.*, 2007). However, their vulnerability to ocean acidification varies between individuals, populations and species (Ries *et al.*, 2009; Calosi *et al.*, 2013a, b). Understanding the likely effects of

ocean acidification requires multi-disciplinary research into long-term response to rising $p\text{CO}_2$ levels (Hilmi *et al.*, 2012). Most studies have shown adverse effects of ocean acidification on sea urchins; however, individual species response is not as clear as first assumed (*Strongylocentrotus droebachiensis*: Siikavuopio *et al.*, 2007; Dupont *et al.*, 2012; *Arbacia lixula*: Hall-Spencer *et al.*, 2008; Calosi *et al.*, 2013a). Most of this research has been carried out using short-term experiments that may overestimate responses by failing to account transgenerational effects, or acclimation and adaptation (Dupont *et al.*, 2012; Pespenti *et al.*, 2013). Acclimation is certainly possible as genes associated with biomineralization and calcification can be affected in ocean acidification simulations (O'Donnell *et al.*, 2009; Martin *et al.*, 2011; Kurihara *et al.*, 2012).

Sea urchins have high Mg-calcite endoskeletons that may be corroded in acidified conditions since calcite solubility increases with Mg-content (Morse *et al.*, 2006; McClintock *et al.*, 2011). LaVigne *et al.* (2013) found that the skeletal composition of adult *Strongylocentrotus purpuratus* was robust to spatial gradients and predicted future changes in carbonate chemistry, although the larvae were affected. As

a follow up to that study, we assess physical and chemical changes in two species of common Mediterranean echinoids (*Paracentrotus lividus*, *Arbacia lixula*) at a shallow-water vent site where organisms are potentially exposed to naturally elevated CO₂ during all stages of their life history. We consider: (1) What is the effect of decreased pH on the abundance of *P. lividus* and *A. lixula*? (2) Is the physical structure of the mature sea urchin test affected? (3) Is the calcite elemental composition affected? We observed the calcification and distribution of sea urchins along gradients of pCO₂ to assess how they may be affected by ocean acidification.

Materials and Methods

Sample sites and study period

Methana is a hydrothermally active peninsula located at the NW terminus of the Hellenic Volcanic Arc on the coast of the Peloponnesus, Greece (37°38'N, 23° 22'E) where there are numerous CO₂ seeps (D'Alessandro *et al.*, 2008). Four sites were compared; the first (V0) was at the centre of a seep flanked by sites 200 m East (V1) and 200 m West (V2) with a control site (C), on the Southern Attica peninsula (37°39'15"N, 24°01'00"E) well away from the influence of any volcanic seeps (Fig. 1). Sampling took place during May and September 2012; in May, sea urchins were collected for analysis of skeletal structure and mineralogy. In both sampling periods abiotic parameters (pH, TA (Total Alkalinity), temperature, and salinity) were measured. To measure pH a calibrated meter was used at each site (YSI 556 MPS, three-point calibration, NBS scale). Temperature and salinity were also measured alongside pH and samples were taken at various times throughout the day over the two sampling cruises (Sept 2012 (acidified site n = 43, reference

site n = 3) and May 2012 (acidified site n = 17, reference site n = 4). Mean pH ± SE was calculated based on hydrogen ion concentrations (Table 1). Total Alkalinity was also measured from a water sample taken from each site on both sampling dates using an AS-Alk 2 Total Alkalinity Titrator (Apollo SciTech Inc, Bogart, GA, USA). Other seawater carbonate chemistry parameters were calculated using CO2 SYS software (Lewis & Wallace, 1998; Table 1).

In situ transects and collection of individuals

Abundance surveys were carried out to measure the density of *P. lividus* and *A. lixula* at each site. Transects were 5 m x 1.5 m at a depth of 1-3m. A minimum of 5 transect repeats for each separate species were carried out at each site during each sampling period (n= 55 per species). Five individuals of each species, from each site, were also collected for trace element composition analysis and for visual inspection of dissolution. Mature adults with a test size diameter greater than 5 cm were collected from the sample stations; *P. lividus* was absent at V0.

X-Ray Fluorescence (XRF) Analysis

Specimens were pre-cleaned in Milli-Q (18.2MΩ) water for 12 hours before being air-dried. Individuals were then cleaned via oxidation in 30% hydrogen peroxide for 48 hours, and later via mechanical cleaning to remove organic material contained within the matrix. Samples were then dried at 70° C for 48 hours. Spines were removed and the test finely ground to less than 500 μm using an acid cleaned pestle and mortar before secondary cleaning with hydrogen peroxide (30%) to remove any remaining traces of non-lattice bound material. The method was developed in studies of corals, sand dollars, and foraminifera; hydrogen

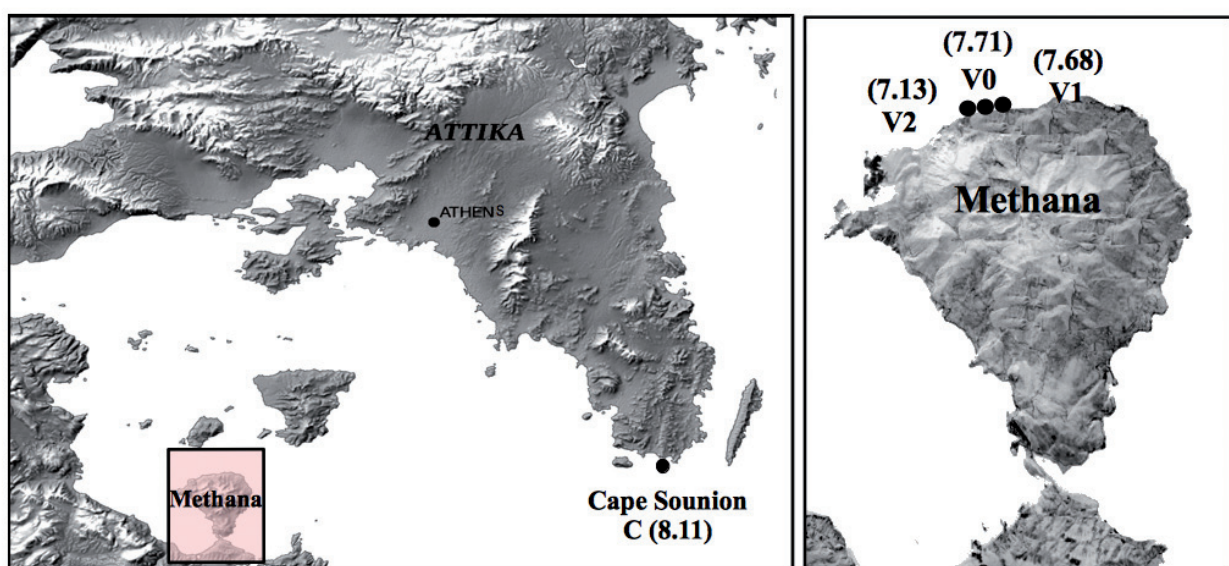


Fig. 1: Map showing four study sites within the Southern Attica peninsula, Greece. The Methana sites were spaced approximately 200 m apart. The Sounion control site was selected because it had a similar algal and predator assemblage, but was outside the area influenced by low pH. Mean pH is indicated in brackets.

Table 1. pH, temperature, salinity, carbon dioxide partial pressure, Total Alkalinity, bicarbonate and carbonate concentration, calcite saturation state and aragonite saturation state measured at four sites in Greece. All variables calculated using CO2 SYS software are highlighted with asterisk. Values shown \pm SE.

| Site | PH NBS | T °C | S ppt | *pCO ₂ µatm | TA mmol kg ⁻¹ | *CO ₃ ²⁻ µmol kg ⁻¹ | *HCO ₃ ⁻ µmol kg ⁻¹ | *Ω calcite | *Ω aragonite |
|------|-------------|------------|------------|---------------------------|-----------------------------|---|---|---------------|-----------------|
| C | 8.11 ± 0.03 | 21.1 ± 0.1 | 39.4 ± 0.1 | 615 ± 35 | 2.66 ± 0.01 | 241 ± 7 | 2194 ± 17 | 5.54 ± 0.17 | 3.79 ± 0.10 |
| V0 | 7.48 ± 0.07 | 20.6 ± 0.1 | 39.2 ± 0.6 | 2700 ± 1036 | 2.89 ± 0.02 | 125 ± 11 | 125 ± 11 | 2.89 ± 0.26 | 1.95 ± 0.18 |
| V1 | 7.75 ± 0.07 | 20.6 ± 0.1 | 39.3 ± 0.6 | 1398 ± 294 | 2.81 ± 0.01 | 147 ± 18 | 2422 ± 43 | 3.40 ± 0.41 | 2.26 ± 0.28 |
| V2 | 7.50 ± 0.10 | 20.5 ± 0.1 | 39.3 ± 0.6 | 2541 ± 1177 | 2.79 ± 0.02 | 138 ± 19 | 2444 ± 45 | 3.19 ± 0.43 | 2.12 ± 0.29 |

peroxide is considered suitable for the removal of organic material in preparation for trace element analysis (Watanabe *et al.*, 2001; Russell *et al.*, 2004; Ehrlich *et al.*, 2011). Specimens were collected *in situ* alive and stored in refrigerated containers pre-cleaned with Milli-Q (18.2MΩ) water before analysis. We then assumed that all remaining inner matrix material was organic and interlaced within the skeletal structure and thus suitable for XRF analysis. For trace element analysis (As, Br, Ce, Mn, Mo, Ni, Rb, Sn, Sr, Te, Th, and Zn), a minimum of 3 g of dried sample was mixed with 1.25 g of wax (Hoechst Wax-C) to assist in the binding of the material. Powdered samples were pressed into a pill format within a 31 mm aluminium cup and used for analysis with a Philips PW-2400 X-Ray Fluorescence machine.

Previous studies have assessed the precision and

accuracy of XRF determination of the major and trace elements used by this method and have calculated the limits of determination of a method (LDM), as an estimation of how well an analytical method can repeat a given result within a 95.4% confidence limit, including any sample preparation, instrument and counting statistic errors (Rousseau, 2001; Karageorgis *et al.*, 2005). Relative uncertainty associated with the use of this method in comparison to the international reference material PACS-2 has previously been calculated for major and trace elements using 10 replicates (Table 2), and all values were found to be satisfactory for the analytical method applied (Karageorgis *et al.*, 2005). It was not possible to analyse all samples due to equipment failures, but 32 out of 35 specimens were successfully analysed for trace elements.

Table 2. Values for calibration range, limit of determination (LDM) and relative uncertainty for major (%) and minor (µg/g) elements analysed with the XRF method (Note: Table retrieved from Karageorgis *et al.* (2005). Copyright 2005 by Elsevier. Reprinted with permission.

| Component | Calibration range (%) | LDM (%) | PACS-2 given conc. (%) | PACS-2 measured conc. (%) | Relative uncertainty (%) |
|--------------------------------|--------------------------|------------|---------------------------|------------------------------|-----------------------------|
| SiO ₂ | 0–80 | 0.61 | 59 ^a | 58.01 | 1.68 |
| Al ₂ O ₃ | 0–25 | 0.12 | 12.50 | 12.03 | 3.78 |
| TiO ₂ | 0–2 | 0.01 | 0.739 | 0.728 | 1.49 |
| Fe ₂ O ₃ | 0–12 | 0.07 | 5.85 | 5.96 | 1.88 |
| K ₂ O | 0–6 | 0.02 | 1.49 | 1.52 | 1.74 |
| Na ₂ O | 0–6 | 0.06 | 5.00 | 4.89 | 2.14 |
| CaO | 0–50 | 0.04 | 2.75 | 2.81 | 2.22 |
| MgO | 0–10 | 0.03 | 2.44 | 2.39 | 1.97 |
| P ₂ O ₅ | 0–1 | 0.01 | 0.220 | 0.227 | 3.40 |
| | (µg/g) | (µg/g) | (µg/g) | (µg/g) | (%) |
| V | 0–300 | 3 | 133 | 143 | 7.29 |
| Cr | 0–500 | 4 | 90.7 | 94.4 | 4.07 |
| Mn | 0–5000 | 4 | 440 | 455 | 3.51 |
| Co | 0–80 | 2 | 11.5 | 11.5 | 0.00 |
| Ni | 0–500 | 2 | 39.5 | 38.5 | 2.48 |
| Cu | 0–450 | 4 | 310 | 326 | 5.14 |
| Zn | 0–1100 | 12 | 364 | 344 | 5.39 |
| As | 0–70 | 2 | 26.2 | 28.0 | 6.95 |
| Sr | 0–3200 | 2 | 276 | 300 | 8.96 |
| Mo | 0–35 | 1 | 5.43 | 5.6 | 3.13 |
| Ba | 0–3100 | 54 | – | 802 | – |
| Pb | 0–250 | 4 | 183 | 188 | 2.74 |

^a=Low quality value.

Scanning Electron Microscope/EDX preparation

Sea urchin plates and spines were prepared for SEM/EDX analysis. Where possible, the same plates were taken for analysis (8 plates above the oral plate layer), making an assumption of homogeneity, and each spine was sliced into three sections to view the central structure. Specimens were coated in carbon by a Baltec CED 030 carbon thread evaporator, reducing picture clarity in comparison to a gold coating but enabling EDX analysis. A Philips XL20 SEM and JEOL 6610 LVSEM were used to take photographs at scales of 500, 200, 100 and 10 micrometres (working distance 10mm) for the plates and where possible 200 and 100 micrometre scales for the spines of each individual. Plate photographs were taken of approximately the same area around the primary pore site of the plate for comparison purposes. EDX analysis of major elements (Ca, Mg, Na, S, and Cl) was performed by the JEOL 6610 LVSEM using Oxford Instruments AzTEC EDS and an average of 10 data points were taken for each sample site to allow for anomalies in data measurements.

Statistical analysis

Data were checked for normality (Kolmogorov-Smirnov), and transformed in cases of non-parametric data (proportion and log transformation). For pH, temperature and salinity comparisons between all four sites ANOVA and suitable post-hoc tests (Tukey) were used for variance comparisons. Data that failed tests for normality (Kolmogorov-Smirnov) and equal variance (Levene test) were analysed by the Kruskal-Wallis one way-analysis and individual Mann-Whitney U tests were used as a post-hoc test. After analysis of abiotic parameters and site reclassification (see results section), the control and experimental sites of the study were compared using a two-sample *t* test for parametric data or a Mann-Whitney U test on non-parametric data. Where multiple tests were carried out, a Bonferroni adjusted *p* value was used to compensate for increased Type-1 errors.

Results

Abiotic parameters/site suitability

The control site had a significantly higher pH than the seep stations (Kruskal Wallis test, $H_4=30.034$, $P=0.000005$) but the seep sites had similar pH. V0 showed no difference to V1 (Mann Whitney U Test, U_{377} , $P=0.1139$), V1 showed no statistical difference to V2 (Mann Whitney U Test, $U_{183.5}$, $P=0.9613$) and V2 showed no difference to V0 (Mann Whitney U Test, $U_{391.5}$, $P=0.1588$) (Table 1). With regards to spatial and temporal variability, we experienced large fluctuations in pH at the sites around the Methana seep in comparison to the control site, as shown by the standard deviation of each site ($STD_C=0.08$, $STD_{V0}=0.26$ $STD_{V1}=0.25$ $STD_{V2}=0.32$). Our study would benefit from long-term time series of pH fluctuations but this information is currently unavailable. As regards to other abiotic parameters, temperature was not significantly different between the sites, but the control had a lower salinity than V2 (Kruskal Wallis test, $H_4=12.93448$, $P=0.0116$, Mann Whitney U Test, $W_{40.5}$, $P=0.0072$). The rest of the sites had no significant differences in temperature and salinity.

Due to a relatively limited number of specimens from the seep sites (V0, V1, and V2) and no significant differences in pH measurements, we pooled data from all stations with a lower pH for density and element analysis comparisons, thus creating two sites:

- Normal pH (Reference site control)
- Acidified water (Replicate CO₂ seep sites)

Site abundances

A. lixula has a similar abundance between the two sites (Mann-Whitney test, $U_{95.5}$, $P=0.25$ (Fig. 2A) but *P. lividus* was more abundant at the control site than in the seep area (Mann-Whitney test, U_{18} , $P<0.00$) (Fig. 2B).

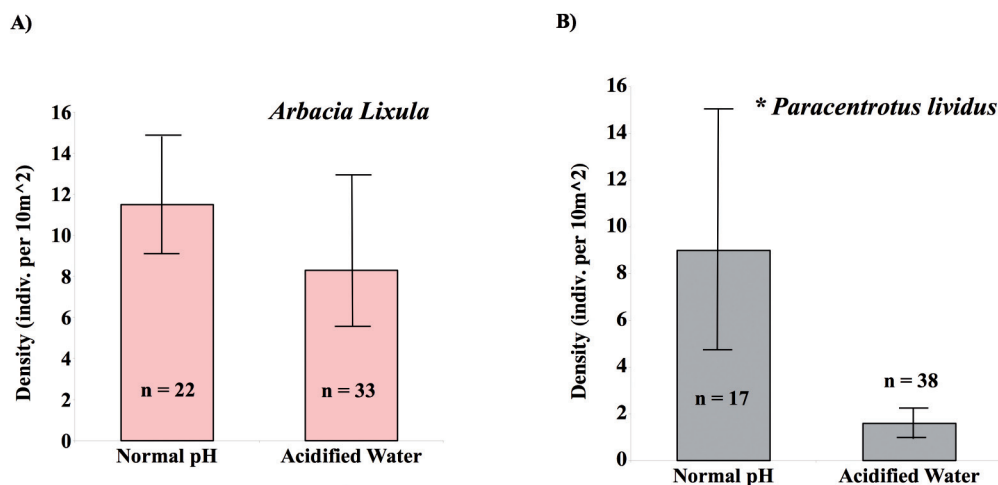


Fig. 2: Bar graphs showing mean abundance and 95% confidence interval for A) *A. lixula* and B) *P. lividus* for a control site and areas experiencing low pH. Statistical differences between sites are indicated by an asterisk.

Skeletal structure

SEM (Scanning Electron Microscope) photographs were analysed for differences in skeletal structure between the controls and low pH stations. No obvious differences are noted with respect to the formation of the spines for both species (Fig. 3G, H). However, some limited differences were detected under high magnification of the ossicle pores for *A. lixula*. The stereom pores were less uniform in shape (Fig. 3A, E) and had increased inner matrix pores (Fig. 3C) at the acidified sites compared to the control site (Fig. 3B, D, F). There were also signs of degradation in the calcium carbonate skeleton (Fig. 3A, E) at the acidified sites.

Element analysis

As, Br, Ca, CaO, Ce, Cl, Cr, Cu, Mg, Mo, Na, Ni, Rb, S, Sn and Th, were not significantly different between study sites (Table 3). For *A. lixula*, manganese was the only element that differed statistically between the sites; the highest concentrations were found in the tests of organisms collected from the area with lower pH (Independent t-test, $t=5.015$, $P=0.007$) (Fig. 4A). For *P. lividus*, Mn was also found in higher concentrations in the acidified water (Independent t-test, $t=4.313$, $P=0.049$) (Fig. 4B), as was strontium (Independent t-test, $t=5.603$, $P=0.005$) (Fig. 4C). Zinc, however, was significantly less abundant in the skeletal structure of organisms collected from low pH areas (Independent t-test, $t=4.429$, $P=0.004$) (Fig. 4D) for *P. lividus*.

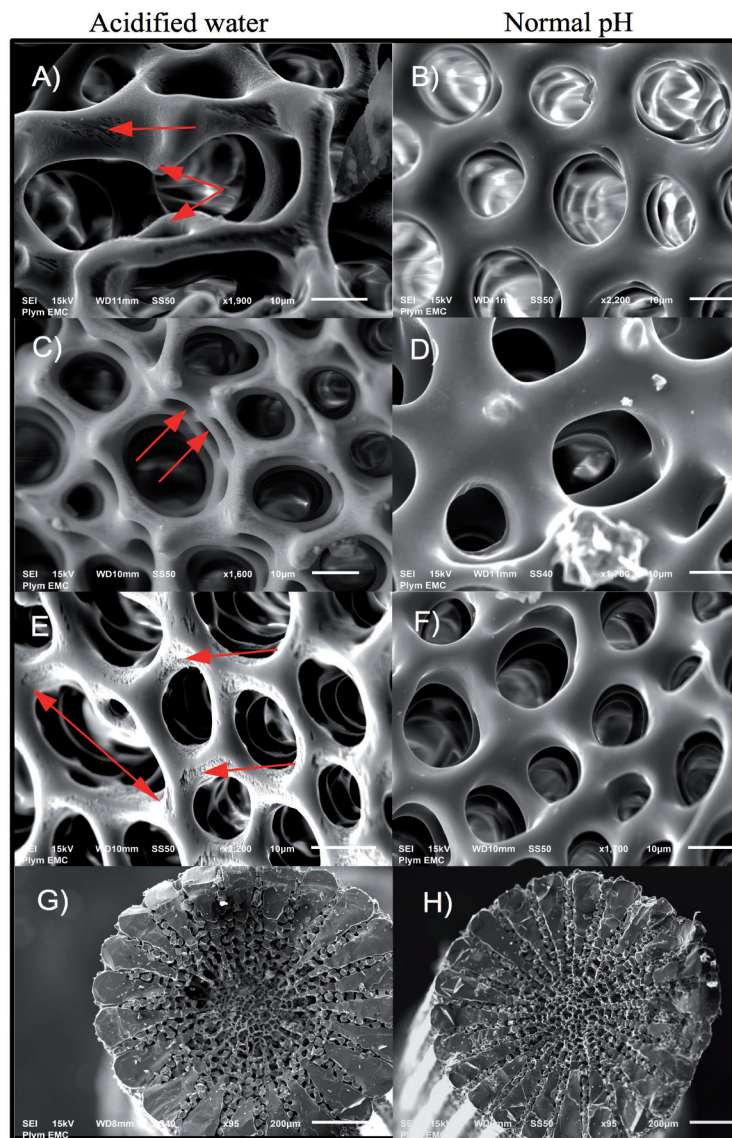


Fig. 3: SEM photographs of individuals collected from areas of normal pH and acidified water. All scale bars shown individually. Highlighted arrows indicate obvious features mentioned in text. A= *A. lixula* from site V0. Ossicles magnification 1900x, WD (Working Distance) 11mm; B= *A. lixula* individual from control site. Ossicles magnification 2200x, WD 10mm; C= *A. lixula* individual collected from site V0. Ossicles magnification 1600x, WD 10mm; D= *A. lixula* individual collected from site V0. Ossicles magnification 2700x, WD 10mm; E= *P. lividus* individual collected from site V2. Ossicles magnification 2200x, WD 10mm; F= *P. lividus* individual collected from control site. Ossicles magnification 1700x, WD 10mm; G= *A. lixula* individual collected from site V0. Spine Magnification 95x, WD 8mm; H= *A. lixula* individual collected from the control site. Spine Magnification 95x, WD 8mm.

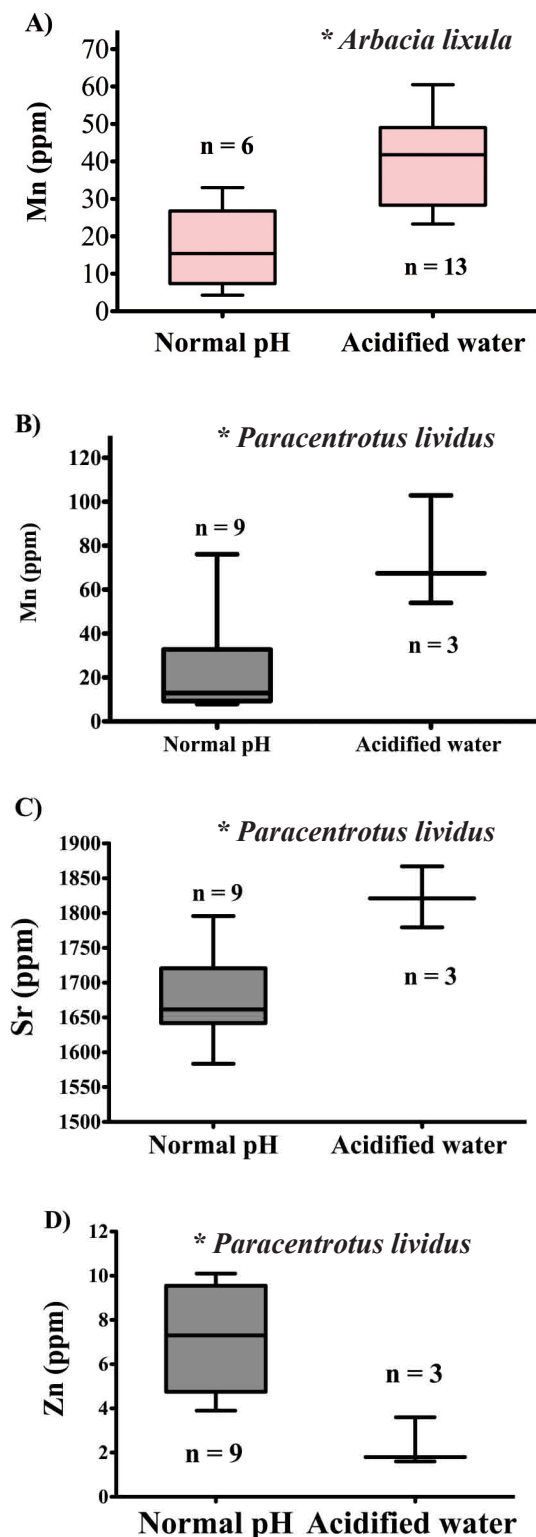


Fig. 4: Boxplots showing significant differences in element composition for normal pH (C) and acidified water (V0, V1 and V2) with median and interquartiles for A) the concentration of Mn in *A. lixula* tests, B) the concentration of Mn in *P. lividus* tests, C) the concentration of Sr in *P. lividus* tests, and D) the concentration of Zn in *P. lividus* tests. All were significantly different between normal pH and acidified water ($P \leq 0.05$).

Discussion

Density distribution

Although early developmental stages of *P. lividus* can tolerate short-term acidification (Martin *et al.*, 2011), the adults showed the same sharp decrease in abundance as that found along other natural CO_2 gradients (Hall-Spencer *et al.*, 2008; Johnson *et al.*, 2012). In contrast, *A. lixula* was more resilient to the acidified conditions, with no statistical differences between densities at reference sites and acidified rocky shore areas. This is in line with the findings of Calosi *et al.* (2013a) who also found that *P. lividus* was more sensitive to naturally acidified waters than *A. lixula*. Such species-specific differences will no doubt influence ecosystem shifts as the oceans continue to acidify.

Calcification

Volcanic seeps show that most calcified organisms, including echinoids, fare badly as $p\text{CO}_2$ levels increase (Hall-Spencer *et al.*, 2008; Fabricius *et al.*, 2011; Johnson *et al.*, 2012; Inoue *et al.*, 2013). Transplantation experiments have shown that acidification differentially affects organisms, with some acclimating to these conditions by up-regulating calcification and others able to protect themselves from dissolution due to the presence of protective layers (Rodolfo-Metalpa *et al.*, 2011). However, species with high Mg-calcite skeletons, such as sea urchins, are thought to be especially vulnerable to increased sea water acidity as this mineral form of carbonate is easily dissolved in corrosive waters and the lowered pH can be detrimental to metabolism and reproduction (Morse *et al.*, 2006; Andersson *et al.*, 2008; McClintock *et al.*, 2011; Stumpp *et al.*, 2011, 2012). Our SEM photographs (Fig. 3) indicate some dissolution to the stereom, in line with widespread dissolution of tests recorded at other CO_2 vents (Hall-Spencer *et al.*, 2008) and the dissolution of larval echinoderm spicules from lowered pH (Pagano *et al.*, 1985; Kurihara & Shirayama, 2004; Byrne, 2012). Reduced carbonate ion availability causes an increase in energy required for the precipitation of calcium carbonate. Skeletogenesis has been shown to be less prevalent under elevated CO_2 conditions and an increased biological effort is needed to form the high levels of skeletal organisation in adult sea urchin species (O'Donnell *et al.*, 2009). The high Mg-calcite skeletal structure of sea urchins is 30 times more soluble than calcite structures (Politi *et al.*, 2004). Therefore, decreased calcification rates and carbonate saturation states could result in a decrease in test size and thickness (Ries *et al.*, 2009). Our SEM studies indicate that the effect of dissolution was stronger in *A. lixula* than *P. lividus*, although this result was difficult to quantify.

Table 3. Element concentration of skeletal structure listed in either parts per million or % weight for *P. lividus* and *A. lixula*, sea urchin test statistics dependant on statistical test used; significantly different results ($P \leq 0.05$) are highlighted in bold.

| Skeletal element | <i>Paracentrotus lividus</i> | | | | <i>Arbacia lixula</i> | | | |
|------------------|------------------------------|----------------------|----------------|--------------|-----------------------|----------------------|----------------|--------------|
| | Normal pH mean | Acidified water mean | Test Statistic | P value | Normal pH mean | Acidified water mean | Test Statistic | P value |
| As (ppm) | 2.20 | 4.0 | $t = 1.264$ | 0.327 | 1.40 | 1.24 | $t = 0.190$ | 0.864 |
| Br (ppm) | 10.14 | 3.87 | $t = 2.421$ | 0.052 | 15.63 | 5.11 | $t = 4.066$ | 0.51 |
| Ca (% weight) | 53.11 | 50.79 | $t = 0.430$ | 0.685 | 53.83 | 49.45 | $t = 1.072$ | 0.315 |
| CaO (ppm) | 933956.53 | 978720.25 | $t = 2.006$ | 0.257 | 987881 | 966840.92 | $t = 0.401$ | 0.705 |
| Ce (ppm) | 10.64 | 8.03 | $t = 1.166$ | 0.332 | 5.33 | 7.97 | $t = 4.179$ | 0.360 |
| Cl (% weight) | 0.51 | 0.11 | $U = 20.00$ | 0.954 | 0.25 | 0.23 | $U = 34.00$ | 0.926 |
| Cr (ppm) | 9.44 | 9.03 | $t = 0.284$ | 0.795 | 8.30 | 8.58 | $t = 0.198$ | 0.858 |
| Cu (ppm) | 1.54 | 3.37 | $t = 1.236$ | 0.315 | 3.03 | 2.92 | $t = 0.352$ | 0.730 |
| Mg (% weight) | 3.58 | 3.70 | $t = 0.614$ | 0.554 | 3.41 | 3.70 | $t = 1.788$ | 0.100 |
| Mn (ppm) | 11.66 | 74.77 | $t = 4.313$ | 0.049 | 11.80 | 40.43 | $t = 5.015$ | 0.007 |
| Mo (ppm) | 0.56 | 0.50 | $t = 0.602$ | 0.569 | 0.57 | 0.38 | $t = 1.551$ | 0.174 |
| Na (% weight) | 0.42 | 0.45 | $U = 24.00$ | 0.953 | 0.46 | 0.40 | $t = 0.798$ | 0.446 |
| Ni (ppm) | 1.16 | 0.33 | $t = 1.109$ | 0.322 | 0.27 | 0.38 | $U = 18.00$ | 0.829 |
| Rb (ppm) | 7.56 | 7.90 | $t = 0.862$ | 0.424 | 7.77 | 7.36 | $t = 1.214$ | 0.297 |
| S (% weight) | 0.51 | 0.48 | $U = 19.00$ | 0.513 | 0.59 | 0.61 | $U = 30.00$ | 0.643 |
| Sn (ppm) | 1.14 | 1.97 | $t = 0.622$ | 0.581 | 1.10 | 1.55 | $U = 17.5$ | 0.767 |
| Sr (ppm) | 1646.72 | 1822.60 | $t = 5.603$ | 0.005 | 1692.5 | 166.3023 | $t = 0.450$ | 0.692 |
| Te (ppm) | 2.42 | 2.33 | $t = 0.120$ | 0.911 | 2.10 | 3.13 | $t = 1.002$ | 0.401 |
| Th (ppm) | 26.52 | 29.43 | $t = 2.022$ | 0.120 | 26.33 | 26.40 | $t = 0.207$ | 0.852 |
| Zn (ppm) | 7.02 | 2.33 | $t = 4.429$ | 0.004 | 3.67 | 3.55 | $t = 0.194$ | 0.855 |

Skeletal mineralogy

We found differences between the elemental test compositions for both species grown under different $p\text{CO}_2$ levels. The incorporation of trace elements into the skeletal structure in response to low pH environments is possible due to the high Mg-calcite structure of sea urchin skeletons, (Dodd, 1967). Sea urchins exhibit a range of ion precipitation and calcification rate responses when exposed to low pH environments but this varies between populations and species (Ries, 2011; Byrne *et al.*, 2013; Courtney *et al.*, 2013; Pespeni *et al.*, 2013). Ionic substitution of the calcite skeletal structure occurs throughout all sea urchin life history stages, including a transient highly soluble, amorphous calcium carbonate stage (Wilt, 2002; Politi *et al.*, 2008). During biomineralization, element incorporation (predominantly Mg) occurs at active sites of the organic matrix and is dependent on temperature (Chave, 1954); seawater composition/saturation state (Ries, 2009); and precipitation rate (Kinsman & Holland, 1969; Carpenter & Lohmann 1992).

Our results showed statistical differences in the concentrations of three skeletal trace elements (zinc, strontium and manganese) between acidified and control sites. Our speculations about the mechanisms and consequences of altered trace element composition due to ocean acidification warrant further study.

Zinc

The concentration of zinc in the test of *P. lividus* was 66% lower at sites with a lower pH (Fig. 4D). Zinc is involved in many metabolic pathways: zinc-containing proteases degrade extracellular matrix proteins and play a role in matrix protein metabolism; cell migration; apoptosis; membrane fusion and the release/activation of growth factors (Poustka *et al.*, 2007; Mann *et al.*, 2008). How zinc concentrations in sea urchin tests affect metabolic pathways is not yet fully understood. Zinc is also essential for reproduction, generally present in high concentrations of several species of female sea urchin gonads during reproduction. A large amount of zinc is expected to be required in female gonads for metabolic processes occurring during cell divisions after fertilization (Guillou *et al.*, 2000; Ahn *et al.*, 2009). Reproductive status might explain the lower levels of zinc expressed within the skeletal matrix for *P. lividus* but we did not study this aspect. The influence of diet variations is also an important consideration since *P. lividus* feed on fleshy macroalgae (Wangensteen *et al.*, 2011), which shift in community composition along CO_2 gradients (Hall-Spencer *et al.* 2008; Johnson *et al.*, 2012). Thus, there is plenty of scope for follow-up work to determine why zinc levels differed significantly between sites.

Strontium

The strontium concentration of *P. lividus* skeletal structure increased by 11% (Fig. 4C), with no apparent changes to the skeletal Sr concentration of *A. lixula*. The similar ionic radius of Mg^{2+} with Ca^{2+} means magnesium is easily adsorbed into the calcite structure, thus distorting the crystal lattice and enabling the incorporation of larger Sr ions into the skeletal structure (Mucci and Morse, 1983). The relationship between low pH and Sr incorporation has previously been shown in a Southern California population of *Strongylocentrotus purpuratus* where larvae were cultivated under lowered pH conditions (7.73). As in this study, no statistical increases of Mg were measured. However, the results did show an 8% increase in skeletal Sr concentration (LaVigne *et al.*, 2013). An increase in Sr incorporation may be an indicator of increased mineral precipitation rate at calcification sites, given that a positive linear relationship is evident between incorporation of Sr and the precipitation rate of sea urchins (Kinsman and Holland, 1969; Carpenter and Lohmann 1992).

Several sea urchin species have the ability to up-regulate specific genes that adjust skeletogenic pathways with the purpose of sustaining precipitation rates in low pH environments (Evans *et al.*, 2013) or biomineralization and ion homeostasis (Pespeni *et al.*, 2013). *Paracentrotus lividus* is able to up-regulate genes thought to be involved in development and biomineralization when exposed to low pH conditions (Martin *et al.*, 2011). This suggests an increase of the biomineral precipitation rates of *P. lividus* in response to low pH environments. The absence of change in the skeletal Sr composition for *A. lixula* also indicates that physiological stress responses to low pH conditions are species-specific (Fig 4.).

Manganese

Manganese was the only element that dramatically increased for both species within the acidified environment (243% increase of Mn in *A. lixula* and 541% increase for *P. lividus*) (Fig 4. A, B). In the Mg-calcitic skeletons of echinoids, Mn can also be incorporated in an almost Mg-free calcite structure (“main-structure”) and in a magnesite-like “(sub)-structure” (Binyon, 1972; Richter *et al.*, 2003) as a ‘foreign’ ion. The incorporation of foreign ions into the crystal lattice substantially increases solubility (Berner 1975; Mucci and Morse, 1983; Davis *et al.*, 2000) and incorporation of Mn^{2+} frequently leads to abnormal skeletal growth (Richter *et al.*, 2003). In a recent study by Pinsino *et al.* (2011), *P. lividus* was exposed to high levels of Mn from fertilization. This produced a number of embryos without skeletons, due to the disruption of signalling pathways during skeletogenesis.

It is noteworthy that the skeletons of *A. lixula* were less affected than those of *P. lividus* since foreign ion incorporation is not a passive process in sea urchins

(LaVigne *et al.*, 2013). A similar variation in responses between the two species was found in the maintenance of acid-base balance in response to increased CO_2 environments (Calosi *et al.*, 2013a) thus supporting the suggestion that *A. lixula* is able to maintain better control over skeletal mineralogy and fares better in an acidified environment.

Conclusions

Our knowledge about how organisms may acclimate and adapt to ocean acidification is limited but increasing because areas with naturally elevated levels of CO_2 are being used to draw further conclusions from artificial laboratory conditions (Calosi *et al.* 2013b; Evans *et al.* 2013; Pespeni *et al.* 2013). A sea urchin species-specific response at the Methana CO_2 seep mirrors that observed along other natural CO_2 gradients (Calosi *et al.*, 2013a). *Arbacia lixula* was more tolerant to acidification and its skeletal mineralogy was less affected than *Paracentrotus lividus*; the latter had an inferior ability for ion homeostasis in acidified environments, with a higher incorporation of trace elements into the skeletal structure when exposed to elevated pCO_2 . The conclusions of this study are: 1) the skeletal mineralogy of calcified organisms can be radically altered by ocean acidification and 2) species-specific differences of keystone grazer responses to ocean acidification may have knock-on effects that are expected to alter marine ecosystems.

Acknowledgements

The authors wish to thank the technicians of Plymouth University and the Hellenic Centre for Marine Research for their advice and use of equipment, and especially Cecilia Baggini for providing abiotic data and assistance during field work. We are also grateful to Dr Christos Anagnostou and Dr Theodoros Kanellopoulos for their advice and invaluable expertise. The work was funded by the EC FP7 ‘Mediterranean Sea Acidification in a changing climate’ project (MedSeA; grant agreement 265103).

References

- Ahn, I.Y., Ji, J., Park, H., 2009. Metal accumulation in sea urchins and their kelp diet in an Arctic fjord (Kongsfjorden, Svalbard). *Marine Pollution Bulletin*. 58, (10), 1571-1577.
- Andersson, A.J., Mackenzie, F.T., Bates, N.R., 2008. Life on the margin: implications of ocean acidification on Mg-calcite, high latitude and cold-water marine calcifiers. *Marine Ecology Progress Series*, 373, 265-273.
- Berner, R.A., 1975. The role of Magnesium in the crystal growth of calcite and aragonite from sea water. *Geochimica et Cosmochimica Acta*, 39, 489-504.
- Binyon, J., 1972. *Physiology of echinoderms Vol 49 International*

Series of Monographs in Pure and Applied Biology. Division: Zoology. Pergamon Press, Oxford, 212 pp.

- Byrne, M., 2012. Global change ecotoxicology: identification of early life history bottlenecks in marine invertebrates, variable species responses and variable experimental approaches. *Marine Environmental Research*, 76, 3-15.
- Byrne, M., Lamare, M., Winter, D., Dworjanyn, S.A., Uthicke, S., 2013. The stunting effect of a high CO₂ ocean on calcification and development in sea urchin larvae, a synthesis from the tropics to the poles. *Philosophical Transactions of the Royal Society B*, 368, 20120439.
- Calosi, P., Rastrick, S.P.S., Graziano, M., Thomas, S.C., Baggini, C. *et al.*, 2013a. Distribution of sea urchins living near shallow water CO₂ vents is dependent upon species acid-base and ion-regulatory abilities. *Marine Pollution Bulletin*, 73, 470-484.
- Calosi, P., Rastrick, S., Lombardi, C., de Guzman, H., Davidson, L. *et al.*, 2013b. Adaptation and acclimatization to ocean acidification in marine ectotherms: an *in situ* transplant experiment with polychaetes at a shallow CO₂ vent system. *Philosophical Transactions of the Royal Society B*, 368, 20120444.
- Carpenter, S.J., Lohmann, K.C., 1992. Sg/Mr ratios of modern marine calcite: empirical indicators of ocean chemistry and precipitation rate. *Geochimica et Cosmochimica Acta*, 56, 1837-1849.
- Chave, K.E., 1954. Aspects of the Biogeochemistry of Magnesium I. Calcareous Marine Organisms. *The Journal of Geology*, 62, 266-283.
- Courtney, T., Westfield, I., Ries, J.B., 2013. CO₂-induced ocean acidification impairs calcification in the tropical urchin *Echinometra viridis*. *Journal of Experimental Marine Biology and Ecology*, 440, 169-175.
- D'Alessandro, W., Brusca, L., Kyriakopoulos, K., Michas, G., Papadakis, G., 2008. Methana, the westernmost active volcanic system of the south Aegean arc (Greece): Insight from fluids geochemistry. *Journal of Volcanology and Geothermal Research*, 178, (4), 818-828.
- Davis, K.J., Dove, P.M., De Yoreo, J.J., 2000. The role of Mg²⁺ as an impurity in calcite growth. *Science*, 290, 1134-1137.
- Dodd, J.R., 1967. Magnesium and strontium in calcareous skeletons: a review. *Journal of Paleontology*, 41, 1313-1329.
- Dupont, S., Dorey, N., Stumpp, M., Melzner, F., Thorndyke, M., 2012. Long-term and trans-life-cycle effects of exposure to ocean acidification in the green sea urchin *Strongylocentrotus droebachiensis*. *Marine Biology*, 160, 1835-1843.
- Ehrlich, H., Elkin, Y.N., Artoukov, A.A., Stonik, V.A. *et al.*, 2011. Simple Method for Preparation of Nanostructurally Organized Spines of Sand Dollar *Scaphechinus Mirabilis* (Agassiz, 1863). *Marine Biotechnology*, 13, (3), 402-410.
- Evans, T.G., Chan, F., Menge, B.A., Hofmann, G.E., 2013. Transcriptomic responses to ocean acidification in larval sea urchins from a naturally variable pH Environment. *Molecular Ecology*, 22, 1609-1625.
- Fabricius, K.E., Langdon, C., Uthicke, S., Humphrey, C., Noonan, S. *et al.*, 2011. Losers and winners in coral reefs acclimatized to elevated carbon dioxide concentrations. *Nature Climate Change*, 1, 165-169.
- FAOSTAT, 2013. *Food and Agriculture Organization of the United Nations*, <http://faostat.fao.org/site/357/default.aspx> (Accessed 15 July 2013).
- Guillou, M., Quiniou, F., Huart, B., Pagano, G., 2000. Comparison of embryonic development and metal contamination in several populations of the sea urchin *Sphaerechinus granularis* (Lamarck) exposed to anthropogenic pollution. *Archives of environmental contamination and toxicology*, 39, (3), 337-344.
- Hall-Spencer, J.M., Rodolfo-Metalpa, R., Martin, S., Ransome, E., Fine, M. *et al.*, 2008. Volcanic carbon dioxide vents show ecosystem effects of ocean acidification. *Nature*, 454, 96-99.
- Hilmi, N., Allemand, D., Dupont, S., Safa, A., Haraldsson, G. *et al.*, 2012. Towards improved socio-economic assessments of ocean acidification's impacts. *Marine Biology*, 160, 1773-1787.
- Johnson, V.R., Russell, B.D., Fabricius, K.E., Brownlee, C., Hall-Spencer, J.M., 2012. Temperate and tropical brown macroalgae thrive, despite decalcification, along natural CO₂ gradients. *Global Change Biology*, 18, 2792-2803.
- Inoue, S., Kayanne, K., Yamamoto, S., Kurihara, H., 2013. Spatial community shift from hard to soft corals in acidified water. *Nature Climate Change*, 3, 683-687.
- Karageorgis, A.P., Anagnostou, C.L., Kaberi, H., 2005. Geochemistry and mineralogy of the NW Aegean Sea surface sediments: implications for river runoff and anthropogenic Impact. *Applied Geochemistry*, 20, 69-88.
- Kinsman, D.J., Holland, H., 1969. The co-precipitation of cations with CaCO₃-IV. The co-precipitation of Sr²⁺ with aragonite between 16° and 96°C. *Geochimica et Cosmochimica Acta*, 33, 1-17.
- Kurihara, H., Shirayama, Y., 2004. Effects of increased atmospheric CO₂ on sea urchin early development. *Marine Ecology Progress Series*, 274, 161-169.
- Kurihara, H., Takano, Y., Kurokawa, D., Akasaka, K., 2012. Ocean acidification reduces biomineralization-related gene expression in the sea urchin, *Hemicentrotus pulcherrimus*. *Marine Biology*, 159, 2819-2826.
- LaVigne, M., Hill, T.M., Sanford, E., Gaylord, B., Russell, A.D. *et al.*, 2013. The elemental composition of purple sea urchin (*Strongylocentrotus purpuratus*) calcite and potential effects of pCO₂ during early life stages. *Biogeosciences*, 10, 3465-3477.
- Lebrato, M., Iglesias-Rodríguez, D., Feely, R.A., Greeley, D., Jones, D.O.B. *et al.*, 2010. Global contribution of echinoderms to the marine carbon cycle: CaCO₃ budget and benthic compartments. *Ecological Monographs*, 80, 441-467.
- Lewis, E., Wallace, D., 1998. *Program Developed for CO₂ System Calculations*. Oak Ridge, Tennessee: PCarbon Dioxide Information Analysis Center, Oak Ridge National Laboratory. 38pp.
- Mann, K., Poustka, A.J., Mann, M., 2008. The sea urchin (*Strongylocentrotus purpuratus*) test and spine proteomes. *Proteome Science*, 6, 22.
- Martin, S., Richier, S., Pedrotti, M.-L., Dupont, S., Castejon, C. *et al.*, 2011. Early development and molecular plasticity in the Mediterranean sea urchin *Paracentrotus lividus* exposed to CO₂-driven acidification. *Journal of Experimental Biology*, 214, 1357-1368.
- McClintock, J.B., Amsler, M.O., Angus, R.A., Challener, R.C., Schram, J.B. *et al.*, 2011. The Mg-Calcite composition of Antarctic echinoderms: important implications for predicting the impacts of ocean acidification. *Journal of Geology*, 119, 457-466.
- Miles, H., Widdicombe, S., Spicer, J.I., Hall-Spencer, J.M., 2007. Effects of anthropogenic seawater acidification on acid-base balance in the sea urchin *Psammechinus miliaris*. *Marine Pollution Bulletin*, 54, 89-96.

- Morse, J.W., Andersson, A.J., Mackenzie, F.T., 2006. Initial responses of carbonate-rich shelf sediments to rising atmospheric $p\text{CO}_2$ and “ocean acidification”: Role of high Mg-calcites. *Geochimica et Cosmochimica Acta*, 70, 5814-5830.
- Mucci, A., Morse, J.W., 1983. The incorporation of Mg^{2+} and Sr^{2+} into calcite overgrowths: influences of growth rate and solution composition. *Geochimica et Cosmochimica Acta*, 47 (2), 217-233.
- O'Donnell, M.J., Todgham, A.E., Sewell, M.A., Hammond, L.M., Ruggiero, K. *et al.*, 2009. Ocean acidification alters skeletogenesis and gene expression in larval sea urchins. *Marine Ecology Progress Series*, 398, 157-171.
- Pagano, G., Cipollaro, M., Corsale, G., Esposito, A., Ragucci, E. *et al.*, 1985. pH-Induced changes in mitotic and developmental patterns in sea urchin embryogenesis. I. Exposure of embryos. *Teratogenesis, Carcinogenesis, and Mutagenesis*, 5 (2), 101-112.
- Pespeni, M., Sanford, E., Gaylord, B., Hill, T. M., Hosfelt, J.D. *et al.*, 2013. Evolutionary change during experimental ocean acidification. *Proceedings of the National Academy of Sciences*, 110, 6937-6942.
- Pinsino, A., Roccheri, M.C., Costa, C., Matranga, V., 2011. Manganese interferes with calcium, perturbs ERK signaling, and produces embryos with no skeleton. *Toxicological Sciences*, 123, 217-230.
- Politi, Y., Arad T., Klein E., Weiner S., Addadi L., 2004. Sea Urchin Spine Calcite Forms via a Transient Amorphous Calcium Carbonate Phase. *Science*, 306 (5699), 161-1164.
- Politi, Y., Metzler, R.A., Abrecht, M., Gilbert, B., Wilt, F.H., *et al.*, 2008. Transformation mechanism of amorphous calcium carbonate into calcite in the sea urchin larval spicule. *Proceedings of the National Academy of Sciences*, 105, 17362-17366.
- Poustka, A.J., Kühn, A., Groth, D., Weise, V., Yaguchi, S. *et al.*, 2007. A global view of gene expression in Lithium and Zinc treated sea urchin embryos: new components of gene regulatory networks. *Genome Biology*, 8, R85.
- Richter, D.K., Götte, T., Götze, J., Neuser, R.D., 2003. Progress in application of cathodoluminescence (CL) in sedimentary petrology. *Mineralogy and Petrology*, 79, 127-166.
- Ries, J.B., Cohen, A.L., McCorkle, D.C., 2009. Marine calcifiers exhibit mixed responses to CO_2 -induced ocean acidification. *Geology*, 37, 1131-1134.
- Ries, J. B., 2011. Skeletal mineralogy in a high- CO_2 world. *Journal of Experimental Marine Biology and Ecology*, 403, 1-2, 54-64.
- Rodolfo-Metalpa, R., Houlbrèque, F., Tambutte, É., Boisson, F., Baggini, C. *et al.*, 2011. Coral and mollusc resistance to ocean acidification adversely affected by warming. *Nature Climate Change*, 1, 308-312.
- Rousseau, R.M., 2001. Detection limit and estimate of uncertainty of analytical XRF results. *The Rigaku Journal*, 18, 33-47.
- Russell, A.D., Hönisch, B., Spero, H.J., Lea, D.W., 2004 Effects of Seawater Carbonate Ion Concentration and Temperature on Shell U, Mg, and Sr in Cultured Planktonic Foraminifera. *Geochimica et Cosmochimica Acta*, 68 (21), 4347-4361.
- Sala, E., Boudouresque, C.F., Harmelin-Vivien, M., 1998. Fishing, trophic cascades, and the structure of algal assemblages: evaluation of an old but untested paradigm. *Oikos*, 82, 425-439.
- Siikavuopio, S.I., Mortensen A., Dale, T., Foss, A., 2007. Effects of Carbon Dioxide Exposure on Feed Intake and Gonad Growth in Green Sea Urchin, *Strongylocentrotus Droebachiensis*. *Aquaculture*, 266 (1-4), 97-101.
- Stumpp, M., Hu, M.Y., Melzner, F., Gutowska, M.A., Dorey, N. *et al.*, 2012. Acidified seawater impacts sea urchin larvae pH regulatory systems relevant for calcification. *Proceedings of the National Academy of Science*, 109 (44), 18192-18197.
- Stumpp, M., Wren, J., Melzner, F., Thorndyke, M.C., Dupont, S.T., 2011. CO_2 induced seawater acidification impacts sea urchin larval development I: Elevated metabolic rates decrease scope for growth and induce developmental delay. *Comparative Biochemistry and Physiology Part A: Molecular & Integrative Physiology*, 160 (3), 331-340.
- Wangensteen, O., Turon, X., García-Cisneros, A., Recasens, M., Romero, J. *et al.*, 2011. A wolf in sheep's clothing: carnivory in dominant sea urchins in the Mediterranean. *Marine Ecology Progress Series*, 441, 117-128.
- Watanabe, T., Minagawa, M., Oba, T., Winter, A., 2001. Pre-treatment of Coral Aragonite for Mg and Sr Analysis: Implications for Coral Thermometers. *Geochemical Journal*, (35), 265-269.
- Wilt, F.H., 2002. Biomineralization of the spicules of sea urchin embryos. *Zoological Science*, 19 (3), 253-261.
- Zeebe, R.E., 2012. History of seawater carbonate chemistry, atmospheric CO_2 , and ocean acidification. *Annual Review of Earth and Planetary Sciences*, 40, 141-165.